Mechanical characterization of cement-based materials containing biochar from gasification

**Mechanical characterization of cement-based materials containing biochar from gasification**

Alice Sirico [a,*], Patrizia Bernardi [a], Beatrice Belletti [a], Alessio Malcevschi [b], Enrico Dalcanale [b], Ilaria Domenichelli [b] , Paolo Fornoni [c] , Emanuele Moretti [c]

[a] Department of Engineering and Architecture, University of Parma, Parco Area delle Scienze, 181/A, 43124 Parma, Italy

[b] Department of Chemistry, Life Sciences and Environmental Sustainability, University of Parma, Parco Area delle Scienze, 11/A, 43124 Parma, Italy

[c] Mapei S.p.A., Research & Development, via Cafiero 22, Milano, Italy

* Corresponding author. Tel. +39 0521 905709; fax +39 0521 905924.

E-mail address: alice.sirico@unipr.it

**ABSTRACT**

This study focuses on the influence of biochar – a solid, porous, carbonaceous material product resulting from biomass gasification of wood waste – on mechanical properties of cement mortars. In order to investigate its effectiveness for structural purposes, biochar is added in cement mortar in increasing percentages, up to 2.5% by weight of cement. Experimental findings show that, by including a proper biochar percentage, compressive and flexural strengths comparable to those of control specimens are obtained, with a slight increase in fracture energy. The use of biochar in building materials as carbon sink is also part of a strategy for the development of more sustainable materials within the construction industry, since the dual aim of storing carbon in a stable form in buildings and promoting waste reutilization by increasing the recycling rate could be achieved.

**Keywords:** *biochar, cementitious mortar, concrete, waste, carbon sink, sustainability, mechanical properties, fracture energy, Digital Image Correlation.*

## 1 Introduction

Nowadays, the incorporation of by-product powders, such as fly ash, silica fume and ground granulated blast-furnace slag, is commonly applied for the production of concrete and cementitious materials. In particular, they can be used as mineral additive to enhance the performance of cementitious materials in both fresh state (e.g. by modifying the rheology) and hardened state (e.g. by improving mechanical properties and durability). Moreover, they can be also successfully used as cement replacement, so to reduce the material production costs, and above all the environmental impact of cement production that requires large amounts of energy and produce significant quantities of $CO_2$. However, some concerns have been raised by scientific community about potential adverse effects on human and environmental health due to the presence of toxic metals and radionuclides [1,2].

Within this research field lies the study proposed herein. More in details, this work explores the feasibility of using biochar, a stable form of carbon produced via the pyrolysis or gasification of biomass, in cementitious materials. With respect to the other above-mentioned by-product powders, biochar derived from wood is characterised by a low content of heavy metal, according to the composition of the starting biomass. Its use is fairly widespread in sustainable environmental and agricultural practices, while its application for other purposes is still scanty. Anyway, the physical and chemical properties of biochar suggest that its employment as supply for the building industry could be a viable option. It is indeed known that when it is added to the admixture, dangerous or noxious reactions are hardly to be provoked since its chemical stability and low flammability [3].

This use of biochar could be particularly interesting to the aim of developing innovative “green” cement-based materials, able to provide not only adequate mechanical properties, but also above all environmental benefits connected with the re-cycle of biochar. In environment terms, several targets could be reached. First of all, by adding biochar in different percentages in building materials, carbon can be stored and locked in civil structures for decades (so as to respond to Earth planet emergency

related to climate change), thanks to the ability of biochar to incorporate huge amount of carbon in a stable form in its structure. Moreover, cement and more generally concrete industry is known to have an enormous impact on environment, due to the huge consumption of natural resources needed for concrete production (such as sand and gravel) as well as to the vast amount of emission of carbon dioxide ($CO_2$) released in the atmosphere. This latter is mainly related to the cement production and represents the dominant driver of $CO_2$ released in atmosphere not related to combustion [4]. To this aim, biochar was investigated to be added in mortars [5,6] and in concrete [7] to act as binder to replace cement. However, only very small percentages of replacement can be considered in order to not affect the material mechanical properties, since the high percentage of carbon of biochar tends to reduce the pozzolanic attitude of the particles and to increase the demand of water to obtain a sufficient workability of the admixture. Least but not last, by using biochar in the building industry also the valorization of wastes is favored. Actually, char from pyrolysis and gasification plants is usually disposed as a waste; hence, such waste could be re-valorized as aggregate or even cement replacement, in cementitious materials. In a perspective of a circular economy, the use of biochar as additive in cement-based materials would produce economic opportunities, since its disposal usually represents a cost (even more than 100 €/ton), while at the same time the recycling rate would be increased.

Since the difficulties related to the use of biochar as cement replacement, recent works focused on the feasibility of using biochar as micro-aggregate, with the function of filler, for both cement pastes [8,9] and mortars [10–12]. The pore structure of cementitious materials can be improved by optimizing the dosage of biochar in the admixture, thus potentially leading to enhanced compressive strength, flexural strength, toughness, ductility and durability. Mechanical properties can be also improved by exploiting the water-retention ability of biochar: by saturating its particles before mixing, it is able to release water during the curing of the cementitious specimens as it acts as internal curing agent [13].

The most important indicators to determine biochar application in cement-based materials are its physical and chemical properties. These latter are in turn depending on the type of starting biomass as well as on the treatment plant technology. More in details, the type of thermo-chemical conversion, i.e. pyrolysis or gasification, and the specific features of each production cycle (mainly heating rate, maximum temperature and pressure) significantly influence the key factors that make biochar more or less convenient to be used in cement-based materials. The main parameters are represented by the size and the morphology of biochar particles, pore size distribution and structure, content of pure carbon and silica precursors, as well as release of contaminants [11,3].

The aim of this work is to assess the possibility of using biochar from gasification of forestry wood waste as additive for mortars, as a first attempt to develop eco-friendly "green" concrete, with comparable (or even better) physical-mechanical properties than other similar materials already used in building/construction industry. To date, few research works consider this possibility and, to the knowledge of the Authors, the feasibility of adopting biochar derived from gasification, instead from pyrolysis, was not previously explored. The choice of the starting biomass is related to promote circular economy, since wood wastes come from local forests, as well as to assure a biochar not much influenced by seasonality, in order to guarantee physical and chemical properties rather constant during the year. Moreover, it reflects the nature of the feedstock biomass, which is in this case fairly homogeneous if compared to municipal or industrial wastes, for example.

Since the focus of this study is to valuate a structural application of the material, the mechanical performances of different kinds of mortar added with biochar in percentages up to 2.5% by weight of cement are compared. For each admixture considered, both fresh properties (i.e. consistence and bulk density) and hardened properties (i.e. dry bulk density, flexural and compressive strength, fracture toughness) of the obtained materials are investigated. Moreover, fracture behaviour is also explored through Digital Image Correlation (DIC) technique.

## 2 Materials and methods

### 2.1 Biochar

#### *2.1.1 Production*

The biochar used was produced from a mixture of woodchips of local forests (alder, beech, poplar, chestnut, oak and hornbeam) with a maximum of 20% coniferous species. The biomass was dried up before being subjected to gasification, in order to obtain a moisture content lower than 15%. Then, biochar was produced in a downdraft gasifier ("Spanner-Joos" type SJHV-03). Initially the biomass was subjected to pyrolysis at 200 – 500 °C and its decomposition produced gas, tar and char, which then reacted in an environment characterized by limited supply of oxygen. In more detail, in the combustion zone the volatile products of pyrolysis were partially oxidized, while no combustion of the solid fraction occurred. Eventually, in the reduction zone, the remaining solid fraction was gasified by the gas produced by pyrolysis and by oxidation at a temperature of about 900 °C. Once the process was completed, biochar was obtained: the yield of biochar was about 3-4% by weight of the woodchips.

Since the maximum grain size chosen for biochar addition into mortar was 63.5 μm, as preliminary operation the material was passed through successively smaller screens using a mechanical shaker. In more detail, biochar samples were prepared via progressive dry sieving adapted from ASTM D5158-98 10. Seven U.S. Standard sieves were used (4.7, 2.0, 1.0, 0.50, 0.25, 0.15, and 0.00635 mm). 60 g of biochar were put initially in the 4.7 mm sieve and shaken for 10 min. The procedure was repeated through the remaining sieves until a grain size < 63.5 μm was obtained. This sieved fraction represented about 65% of the total biochar sample. Figure 1 reports the particle size distribution for the sieved biochar, as obtained by adopting a laser diffraction particle size analyzer (Mastersizer 3000) based on laser diffraction and Mie Theory, with size ranging from 0.01 μm to 3500 μm. The results show that about 90% of biochar powder size distribution pattern is less than 38 μm.

### *2.1.2 Physical and chemical analyses*

All physical and chemical analyses reported in the following refer to sieved biochar with grain size < 63.5 μm.

The biochar powder was analysed by means of X-Ray Powder Diffraction (XRPD), to have a first identification of the presence of amorphous and/or crystalline phases. The XRPD data were collected using a PANalytical X'pertPro MPD diffractometer equipped with CuKα radiation (λ=1.54184 Å) in a theta-theta geometry. Samples were continuously scanned in the 2theta range 5-80° with a step size of 0.017° and a collection time of 51 s. Qualitative phase analyses were carried out with the PANalytical X'Pert HighScore Plus (ver. 2.2) search/match software.

Thermal stability can be used to determine biochar stability by assessing the fraction of carbon that can endure the thermal degradation/oxidation and thus obtaining the amount or the relative stability of labile or stable carbon in biochar. Thermo-gravimetric analyses (TGA) were carried out on biochar samples by means of a TG 209F1 Iris instrument (Netzsch, Germany) with a heating program from 30 to 980°C and a heating rate of 5 K/min in Nitrogen atmosphere after three vacuum cycles.

The chemical composition of the material was found with X-ray fluorescence (XRF) on a Bruker S8 TIGER wavelength dispersive spectrometer. The sample ashes at 980°C (69.08 %) were prepared as fused beads.

As concern pH, it was determined in a 1:10 (w/v) mixture of biochar to distilled de-ionized water, with 0.25 g biochar in 5 ml water mixture shaken on an oscillating table at 60 RPM for 1 hour prior to measurement.

Other chemical analyses were performed to assess biochar safety for its use into mortar mix. To this aim, heavy metals and polycyclic aromatic hydrocarbons (PAHs) concentration in biochar was determined.

The PAH analysis was carried out using Gas Chromatography coupled to mass Spectrometry (GC-MS). 5 grams of biochar were extracted with 300 ml of a mix of acetone : hexane = 1 : 1 for 10 hours

with a Soxhlet apparatus; the solvent was then evaporated and weighed. The extracted part was recovered with acetone: hexane = 1 : 1 (1-2 ml), adsorbed on a small silica gel column (5 ml), recovered by washing with 5 ml of acetone: hexane = 1:1 and finally dried. Then a known amount of the extracted sample was recovered with toluene spiked with diphenyl as internal standard, and injected for the PAH analysis (1 μl split mode 1/20 ratio) on a GC-MS instrument (Agilent) equipped with a capillary column (30 m x 0.25 mm i.d. x 0.25 μm film thickness) connected with a 5 m silica precolumn (inner diameter 0.53 mm). MS data were recorded at 70 eV scan mode (with a mass range m/z 41-440). A standard mixture containing 16 common PAH compounds was injected under the same GC-MS conditions to allow identification and quantification on the biochar samples.

In order to quantify the heavy metal content, biochar sample was weighed into the reaction vessel of the microwave; 6 ml of nitric acid, 2.0 ml of hydrogen peroxide and 0.4 ml of hydrofluoric acid were added. The reaction vessel was sealed and placed in the microwave and heated (from room temperature to 190°C) in 15 min. After complete cooling, the reaction vessels were opened and the digestion solution was transferred to in a 50 ml plastic volumetric flask and filled with deionized water. The resulting solution was measured by inductively coupled plasma optical emission spectroscopy (ICP-OES), using SPECTRO CirOS Vision EOP, (SPECTRO Analytical Instruments KG, Kleve, Germany).

### *2.1.3 Results of physical and chemical characterization*

The XRD pattern, reported in Figure 2a, shows the presence of calcite ($CaCO_3$) as main crystalline phase and bütschliite ($K_2Ca(CO_3)_2$), apatite ($Ca_5(PO_4)_3OH$) and portlandite ($Ca(OH)_2$) as minor crystalline phases. This result is consistent with what is already known about the formation of carbon-based phases during the process of gasification. At about 350 C° depolymerisation of lignocellulose occurs resulting in the creation of an essentially amorphous C matrix, whereas the formation of polyaromatic graphene sheets decreases at higher temperatures above 600 C°. There is evidence in

literature [14–16] that the presence of carbonate in the biochar is the main alkaline substance, especially in those biochars generated at the high temperatures. Another possible source of calcite may be due to the addition in the plant of calcium oxide (CaO), which has been used as the sorbent in the gasifier in order to obtain a hydrogen-rich syn-gas, avoiding the cost and efficiency penalty for $CO_2$ post capture.

The biochar thermostability depends on the temperature at which it was generated: indeed as the temperature increases, biochar consists of a more stable form of carbon with higher resistance to heat. According to TGA results, reported in Figure 2b, the thermal profile presents a gradual decreasing slope of biochar thermostability up to about 700°C. The stability profile is very good with a final loss percentage of about 30%, limited to 5% below 700°C. This biochar is therefore perfectly suited as inert material in the mortar mix.

The XRF results are reported in Table 1. The results shows a rich mineralogical composition of biochar especially in Calcium (60.49%) and Potassium (19.25%). The reason behind this high mineral concentration is a consequence of the high gasification temperature that enhanced the rate of degradation of organics and resulting in the accumulation of inorganics contents.

The pH of biochar is greatly affected by the type of feedstocks and by the gasification temperature. Generally, biochar produced from gasification tends to have a liming effect as a direct result of an increasing degree of carbonization. Carbonates are considered as the main alkaline components in biochar. In addition during the pyrolysis process, functional groups such as carboxyl and hydroxyl molecules on the surface of biochar are formed. Additionally, the relative content of the ash, which is also basic in nature, is increased during the process. It has to be also noted that pH-value can be raised by increasing the residence time. Actually pH tended to slowly increase when measures were taken in a time lapse experiment (1 day and 5 days). An initial PH of 10.22 was obtained, while from successive measurements after 1 and 5 days, values equal to 10.88 and 10.95 were obtained, respectively.

Heavy metals and polycyclic aromatic hydrocarbons (PAHs) are of great environmental concern due to their toxic, mutagenic and carcinogenic properties. Several studies [17,18] reported the possible presence, inside biochar particles, of high concentrations of hazardous compounds, particularly heavy metals and PAHs. The presence and concentration of heavy metals reflect the kind of initial biomass used for producing biochar. The carbonization process during gasification transforms organic molecules of wood and cellulose materials into carbon, or carbon-containing residues, which are often aromatic in nature (PAH) and can be adsorbed onto biochar surfaces. In this context, the presence of heavy metals and PAHs in the analysed biochar sample was valuated to avoid environmental and human health risks as well as to predict their roles in the possible toxicity of cementitious materials.

Overall the GC-MS analyses showed that the PAHs of biochar were lower the limit of detection (LOD=0.05mg/kg), except for Phenanthrene, which presents a value of 0.25 mg/kg. Anyway, the total PAH content in the biochar was under the established threshold of environmental biosafety, thus it was considered safe for the following experiments.

The heavy metal content in the biochar is given in Table 2. These values can be considered safe and in line with the average values for additions in concrete known in literature [19], also keeping in mind that biochar was added in percentages up to 2.5% by weight of cement.

### 2.2 Mix design definition and preparation of biochar-added cementitious specimens

Three different admixtures were prepared in order to evaluate the influence of biochar addition on mechanical properties of mortar and concrete. Each admixture was made by an ad-hoc mix design, characterized by a specific type of cement, water-cement (W/C) ratio and granulometric composition. In more detail, the admixture denoted as “A” in Table 3 represents a plastic mortar containing one part by mass of cement I 52.5 R and three parts by mass of CEN Standard sand conforming to EN 196-1 [20], while the water-cement ratio is equal to 0.42. Mortar mixes denoted as “B” and “C” in Table 3 try to simulate the effects related to the addition of biochar in concrete; hence, they contain

aggregates with maximum diameter of 8 mm. The grain size distribution of the aggregates in terms of cumulated sieve residue percentage vs. squared mesh size is reported in Table 4. In more detail, mix B, prepared with cement II A-LL 32.5 R and with a water-cement ratio of 0.55, aims to simulate a ready-mix concrete, while mix C – prepared with cement I 42.5 R and with a water-cement ratio of 0.40 – a mixture for precast concrete. They were designed so as to follow the "method of concrete equivalent mortar" (MBE), originally developed by the Technical Laboratory of Italcementi France [21] and adapted on purpose herein. This method is based on the use of the same water-cement ratio and the same sand (or very fine gravel) of the reference concrete, while excluding the amount of gravel. MBE was adopted in the present research so to realize reliable tests on mortars that can also approximately simulate the behavior of concrete. In this way, the influence of biochar on concrete properties can be preliminarily evaluated, identifying the most promising admixtures as a first step to develop sustainable concrete.

As regards the experimental program carried out in this work, biochar was added in each admixture (i.e. A, B and C) in two different dosages: 1% and 2.5% by weight of cement. These percentages were chosen since, as other research works demonstrated (among others, [10,12]), 1% seems to be the optimal quantitative to enhance mechanical properties; moreover, as an attempt an increased percentage value was here investigated equal to 2.5%. As a matter of fact, higher biochar additions presented a high loss of fluidity and the superplasticizer (or water) increase needed to obtain a good workability resulted hardly compatible with practical applications of mortar in the building industry. Moreover, for each mix design, plain specimens without the addition of biochar were cast for control purpose. Accordingly, nine different mortar mixes were prepared, constituted by components in the dosage reported in Table 3. In this Table, the mix nomenclature is formed by a capital letter followed by a digit: letter A, B or C denotes the type of admixture, while the digit refers to the amount of biochar: 0 for plain mortar, while 1 and 2.5 stand for the addition of 1% and 2.5% of biochar by weight of cement, respectively. It can be noted from Table 3 that acrylic polymer based

superplasticizers (produced by MAPEI S.p.A.) were added at slightly different proportions in each mortar mix, in order to obtain enough flowability, since the dosage of biochar influences the flow values. A relatively high water to cement ratio was chosen, especially for mortar B, so as to maximize the beneficial effects due to the addition of biochar particles in the admixture, especially on compressive strength. As reported in [12], biochar, due to its fine grain size as well as to its high absorption capacity, can provide higher compactness of hardened mortars. However, this densification effect was found to be poorer for mortars characterized by a low water-cement ratio, since they are already compact.

To obtain mortar A, the components were mixed in a fully automatic mortar mixer, conforming to EN 196-1 [20]. Water, superplasticizer, cement and biochar (where applicable) were first mixed for 30 s at low speed, then the sand was steadily added during the next 30 s. After additional 30 s of mixing at high speed, the mixer was stopped for 90 s: during the first 30 s the edge of the bowl was scraped and then the admixture was allowed to rest. Finally the mixing was conducted at high speed for 60 s.

A proper mixing procedure was instead developed on purpose for mortars B and C, since they were designed by following MBE. The bowl of a fully automatic mortar mixer was initially wet, then the sand and half of the total water were added. The compound was mixed for 120 s at low speed and then the mixer was stopped for 180 s, by covering the bowl to prevent evaporation. Just before the end of the pause, cement and biochar (where applicable) were added and the admixture was mix for 60 s at low speed; during the last 30 s the remaining water and the superplasticizer were added. After additional 60 s of mixing at high speed, the mixer was stopped for 90 s, while the edge of the bowl was scraped to avoid any deposit of material in the bottom part. Lastly, the mixing was conducted at high speed for 30 s.

The obtained mixtures were cast into 40×40×160 mm prisms through two layers. A jolting table was used for compacting the specimens, by applying 60 jolts per minute for each layer. For each of the

nine admixtures, six specimens were cast, three of them (named in the following as sample a, b, c) for the 7 days testing, and the other three (again denoted with a, b, c) for the 28 days testing. The cast samples, placed in a moist air room, were covered with polythene sheets for 24 hours. After demolding, the specimens were cured in water and then they were air-dried for 24 hours before performing mechanical tests at 7 or 28 days.

### 2.3 Experimental testing on biochar-added cementitious specimens

Both fresh (i.e. consistence and bulk density) and hardened (i.e. dry bulk density, flexural and compressive strength) properties were investigated for each mortar mix.

Consistence of fresh mix A was determined according to EN 1015-3 [22], by measuring (in the two perpendicular directions) the mean diameter of the test samples placed on a flow table after a given number of vertical impacts. The workability was tested on the fresh mortar both immediately and 25 minutes after the end of mixing.

For mortars B and C, the measurement of fresh consistence was carried out by following a procedure developed on purpose, since these mortars were designed by following MBE. A smaller version of the Abrams cone (1:2 scale) was initially wet in its inner part and filled with three layers of mortar, each of them compacted by 25 strokes of pestle. Then the mould was vertically uplifted in 2 sec and the average flow was determined by measuring three different diameters of the slumped mortar for the evaluation of the sample mean diameter, immediately after the end of mixing as well as 20 and 50 minutes later.

Bulk density of fresh and hardened mortar was measured according to EN 1015-6 [23] and EN 1015-10 [24], respectively.

Flexural strength was measured by three-point bending test (3PBT) on notched specimens, performed according to JCI-S-001-2003 [25], so as to determine also the fracture energy. 40×40×160 mm prisms were tested on a net span of 120 mm (Fig. 3a). 24 hours prior to testing a notch – 2 mm width and 12

mm depth, i.e. 0.3 the sample depth – was cut at mid-span. The specimens were loaded at mid-span up to failure, by a high precision servo-electric Universal Testing Machine (Instron 8862). Experimental tests were performed under crack mouth opening displacement (CMOD) control, so as to get a stable post-peak response, which enables to determine the fracture energy. The load, measured through a load cell, was function of the increase of CMOD, by setting a clip gauge across the notch (Fig. 3b,c). The test speed was opportunely chosen so as to reach the peak load in about 5 minutes.

During testing, Digital Image Correlation (DIC) was performed to evaluate displacements, strains as well as crack initiation and propagation. This technique, which nowadays is often applied for the characterization of fracture behaviour of brittle-materials (like cementitious composites), needs precise requirements in order to ensure an adequate accuracy of the correlation between the recorded images. A digital camera NIKON D800 (24.3 Megapixel full frame), was placed on a tripod so as to make its axis perpendicular to the surface of the tested sample, while stable lighting conditions were guaranteed (Fig. 3d). The specimen surface was initially smoothed and painted white; next, a speckle pattern consisting of randomly distributed black dots was carefully applied on it through a flicking paint technique, in order to recognize and trace the position of each point of the sample continuously during the test (Fig. 3b). The digital images, which were shot at a speed of one frame every 6 s during testing, were subsequently analyzed by means of the software Ncorr [26], developed in MATLAB environment. The continuous interpolation of the displacement and strain field occurring at the surface of each specimen was performed by assuming that each pixel covered a real area of about $30\times30$ $\mu m^2$.

Compression tests were performed according to EN 196-1 [20] on the two halves of the prisms previously subjected to three-point bending test; hence, 6 specimens were tested for each batch both after 7 and 28 days curing.

## 3 Experimental results and discussion

### 3.1 Fresh properties

The influence on flow rate was investigated by defining the optimal superplasticizer (SP) dosage (expressed as the percentage ratio between dry content of superplasticizer and cement by weight) required in biochar-added mixes to have the same flowability of plain mortar, for the same water-cement ratio. From the results reported in Table 5 for mortar A, it can be observed that a gradual increase in SP dosage was applied for progressive higher biochar percentages, so to obtain about the same flow diameter for all the admixtures. This effect is related to the porous microstructure of biochar particles that causes water retention. The loss of workability of fresh mortars containing biochar was indeed observed in other researches [5,10,11]. Only for mix A, as further investigation, other biochar-added mixes were prepared by adopting the same amount of cement, sand, superplasticizer of the corresponding plain mortar (as reported in Table 3), but the amount of water was increased so as to obtain about the same flow diameter for all the admixtures. The nomenclature adopted is the same of the corresponding biochar-added mortar, with the addition of the capital letter W at the end. From the values reported in Table 5, it is found that the water required shows an almost linear increase with the biochar percentage. These mixes were excluded from the experimental campaign aimed to evaluate the hardened properties, since a significant strength reduction was expected due to the increased water content.

As regards mix B and C (designed to simulate the effects of the addition of biochar in concrete), Table 6 shows the adopted SP dosage so as to obtain about the same flow diameter of control mix immediately after mixing. Even if the presence of biochar tends to reduce the workability of mortars as time passes, it was found that the addition of 2.5 wt% of biochar offers sufficient flowability also after 50 min.

Fresh density of plain and biochar-added mortars are completely comparable for all the considered mixes (i.e. A, B and C), as shown in Figure 4a. The addition of biochar is found not to significantly influence the density of all fresh mortar mixes considered. This is probably due to two opposite mechanisms: on one side biochar tends to reduce fresh density, due its low density and highly porous nature [10], but on the other side biochar and superplasticizer (which was added at higher percentage with increasing biochar content) have little de-aerating abilities. More in detail, as suggested in [12], biochar, added to mortar at low dosage and thanks to its water-retention capacity, could reduce the amount of free water in fresh mixes responsible for porosity of mortars.

### 3.2 Hardened density

The apparent density of the hardened mortar follows the same trend already observed for fresh density. The addition of biochar in the admixtures up to 2.5 wt% does not lead indeed to a significant difference compared to plain mortars in terms of hardened density both at 7 and 28 days curing. For sake of brevity, only the results at 28 days curing are reported in Figure 4b.

### 3.3 Flexural strength and fracture energy

Flexural strength $f_{ct,fl}$ of mortar specimens is computed from the peak load $P_{max}$ of load (P) - CMOD curve (Figs. 5-7) as:

$$f_{ct,fl} = 1.5\frac{P_{\max} S}{b(d-a)^2} \quad (1)$$

where $S$ is the net span length of the specimen and $a$ the notch depth; moreover, $b$ and $d$ represent the width and depth of the cross section, respectively.

Figures 8a and 8b show the medium values of flexural strength of mortar mix A, B and C, for the different amount of biochar (0, 1 and 2.5 wt%), at 7 and 28 days curing, respectively. Series A0, A1, A2.5 present about the same flexural strength at 7 days, while with the addition of biochar a slight decrease can be observed at 28 days. This reduction of flexural strength at 28 days is in line with

previous findings [10,27,28] stating that biochar tends to produce inhomogeneity of cement paste. Moreover, some research works [12,13] highlight that larger and more numerous air voids could form in hardened mortar in the tensile plane, as a consequence of the addition of biochar, leading to a reduction of the cross section effectively loaded and a stress concentration around voids. The addition of biochar in mix B seems to produce more favourable results, especially at 7 days curing and for the lowest dosage (1 wt%), while the addition of biochar does not lead to significant variation of flexural strength at 28 days. It can be noted that, even if as expected flexural strength increases with curing age for all mortar mixes, this increment is lower for the higher dosage of biochar. This effect could be explained since the addition of biochar generally tends to produce a more beneficial effect on early strength development, because it acts as accelerator additive that leads to early generation of more hydration products, as outlined in the literature [8,11,29]. This trend is not followed by mix C. Anyway, it can be observed from Figure 7a that the samples of the plain series C0 tested at 7 days showed high scatter results. In particular, for sample C0-c a greater load peak than the other two samples was recorded, thus resulting in a higher mean flexural strength value at 7 days, even slightly greater to the corresponding one at 28 days. In any case, the addition of biochar in mortar C seems not to give beneficial effects, since lower flexural strength are reported for both 7 and 28 days curing. The results of 3PBT, reported in Figure 5, 6 and 7, respectively for mortar A, B and C, show that ductility seems not to be significantly influenced by the addition of biochar. The ductility factor, defined as the ratio between the ultimate displacement and that corresponding to the peak load [8], seems about the same for all the considered biochar percentages.

Fracture energy $G_f$ is related to the area $W_0$ under the load-CMOD curves; more in detail, it can be computed by applying the formulation proposed in [25]:

$$G_f = \frac{0.75W_0 + W_1}{A_{lig}}, \tag{2}$$

where $A_{lig}$ is the area of the ligament, i.e. $A_{lig} = b\,(d - a)$, and $W_1$ indicates the work done by specimen deadweight and loading equipment, which in turn can be determined as:

$$W_1 = 0.75\left(\frac{S}{L}m_1 + 2m_2\right)g \cdot CMOD_C \ , \tag{3}$$

being $L$ the total length of the specimen, $g$ the gravitational acceleration and $CMOD_C$ the crack mouth opening displacement at rupture. Moreover, $m_1$ and $m_2$ represent the mass of the specimen and the mass of the instrumentation directly attached on the sample, respectively.

The results, reported in Figure 9, indicate that a slight increase of fracture toughness can be obtain at both 7 and 28 days curing for plastic mortars (corresponding to mix A), if proper percentages of biochar (1 wt%) are used. Similar findings were reported in literature [8,10,11,27], even if the degree of improvement is extremely variable. As suggested in [10], this effect may be related to the intrinsic characteristics of biochar particles, especially in terms of shape and size distribution. The angular shape that leads to more surface area was found to significantly increase toughness [30]; also a granulometry that is able to span over the interfacial transition zone (ITZ) as well as the hydration products could force cracks to paths that are more tortuous [8,28]. Moreover, from the observation of the curves reported in Figure 5 it can be deducted that the data dispersion is higher for the admixtures characterized by the highest biochar percentage, as already outlined by [8], probably due to the difficult to perform a proper dispersion of biochar particles during mixing. An increase of fracture toughness is also shown for mortar B both at 7 and 28 days curing, while for mortar C only at 28 days curing. The different result obtained for mortar C at 7 days could be caused by the high scatter of the curves related to plain concrete (series C0), as already observed for flexural strength.

In order to better analyze the fracture behavior, the horizontal strain field around the notch obtained from DIC processing is analyzed. For sake of brevity, the results are reported (see Fig. 10) only for mortar B, for three samples characterized by different amount of biochar (0, 1 and 2.5 wt%). The tortuosity of the crack path, as well as the observed strain value at different loading stage, is about

the same for all the admixtures, thus the influence of the addition of biochar in this case could not be clearly observed.

### 3.4 Compressive strength

Compressive strength $R_c$ of mortar specimens is computed as follows:

$$R_c = \frac{F_c}{A_c}$$

where $F_c$ represents the maximum load and $A_c$ is the contact area of the auxiliary plates (i.e. 40×40=1600 mm$^2$), placed so that the end face of the specimen overhangs the auxiliary plates by about 10 mm, according to EN 196-1 [20].

Results of the compressive tests are reported in Figures 11a and 11b for all the tested specimens at 7 and 28 days curing, respectively. A slight decrease of compressive strength, which becomes more pronounced as the percentage of biochar increases, can be noticed. A general slight increase in compressive strength is instead found in technical literature [10–13] by the addition of similar percentages of biochar. Nevertheless, as already observed, the physical and chemical properties of biochar particles strongly depend on the type of starting biomass as well as on the treatment plant technology; thus, it is not surprising to find mixed results. As a matter of fact, it is worth noticing that the type of thermo-chemical conversion used in this research, i.e. gasification, is different from pyrolysis, which was used in the other works available in literature.

## 4 Conclusions

This work represents a first attempt for the development of sustainable cementitious materials incorporating biochar, a by-product derived from gasification of wood waste from local forests. The main goal was the characterization of these biochar-added materials from a mechanical point of view, to evaluate if an application in building industry could be promising. Three different cementitious

mixes were investigated: one corresponding to plastic mortar and two admixtures with coarser aggregates simulating a ready-mix concrete and a mixture for precast concrete.

On the basis of the obtained results, some conclusions can be made:

- compressive strength shows a slight reduction with increasing biochar dosage for all mortar mixes with a similar trend both at 7 and 28 days curing;
- flexural strength seems to be little affected by biochar addition, especially for plastic mortars. However, an optimal percentage of 1% by weight of cement can be identified, providing a slight increase of flexural strength in the case of mortar simulating a ready-mix concrete;
- a fracture energy increase in 1% biochar-added specimens can be observed for all the tested admixtures, so confirming the trend suggested by technical literature.

Since mechanical properties are not too negatively affected by biochar addition, its use for the development of new sustainable admixture seems feasible, particularly limiting the dosage to 1% by weight of cement. Environmental and economic benefits can derive from the use of this waste, since biochar is able to store carbon in a stable form in buildings and at the same time it can increase the recycling rate of building sector; last but not least it represents a by-product free of cost.

Anyway, more research is needed to confirm the advantages of the use of biochar from gasification as carbonaceous micro-filler in cementitious materials, as well as to evaluate the key-parameters influencing mechanical properties. As an example, the influence of starting biomass and biochar production process, as well as of biochar pre-treatments, such as grinding or pre-soaking, or even of the curing conditions of the cementitious specimens should be further investigated. Moreover, a further and promising research development could be addressed to explore the use of silica-rich biochar as cement replacement, by considering different starting biomass, such as rice husk or saw dust.

**References**

[1] E. Sharifikolouei, F. Canonico, M. Salvo, F. Baino, M. Ferraris, Vitrified and nonvitrified municipal solid wastes as ordinary Portland cement (OPC) and sand substitution in mortars, Int. J. Appl. Ceram. Technol. (2019). doi:10.1111/ijac.13447.

[2] A. Fucic, L. Fucic, J. Katic, R. Stojković, M. Gamulin, E. Seferović, Radiochemical indoor environment and possible health risks in current building technology, Build. Environ. 46 (2011) 2609–2614. doi:10.1016/j.buildenv.2011.06.020.

[3] S. Gupta, H.W. Kua, Factors Determining the Potential of Biochar As a Carbon Capturing and Sequestering Construction Material: Critical Review, J. Mater. Civ. Eng. 29 (2017) 04017086. doi:10.1061/(asce)mt.1943-5533.0001924.

[4] A. Hasanbeigi, L. Price, E. Lin, Emerging energy-efficiency and CO2 emission-reduction technologies for cement and concrete production: A technical review, Renew. Sustain. Energy Rev. 16 (2012) 6220–6238. doi:10.1016/j.rser.2012.07.019.

[5] W.C. Choi, H.D. Yun, J.Y. Lee, Mechanical properties of mortar containing bio-char from pyrolysis, J. Korea Inst. Struct. Maint. Insp. 16 (2012) 67–74. doi:10.11112/jksmi.2012.16.3.067.

[6] K. Roy, A. Akhtar, S. Sachdev, M. Hsu, J. Lim, Development and characterization of novel biochar-mortar composite utilizing waste derived pyrolysis biochar, Int. J. Sci. Eng. Res. 8 (2017) 1912–1919.

[7] A. Akhtar, A.K. Sarmah, Novel biochar-concrete composites: Manufacturing, characterization and evaluation of the mechanical properties, Sci. Total Environ. 616-617 (2018) 408–416. doi:10.1016/j.scitotenv.2017.10.319.

[8] L. Restuccia, G.A. Ferro, Promising low cost carbon-based materials to improve strength and toughness in cement composites, Constr. Build. Mater. 126 (2016) 1034–1043. doi:10.1016/j.conbuildmat.2016.09.101.

[9] Y.S. Montenegro Camacho, S. Bensaid, B. Ruggeri, L. Restuccia, G. Ferro, G. Mancini, D.

Fino, Valorisation of by-Products/Waste of Agro-Food Industry by the Pyrolysis Process, J. Adv. Catal. Sci. Technol. 3 (2016) 1–11. doi:10.15379/2408-9834.2016.03.01.01.

[10] S. Gupta, H.W. Kua, H.J. Koh, Application of biochar from food and wood waste as green admixture for cement mortar, Sci. Total Environ. 619-620 (2018) 419–435. doi:10.1016/j.scitotenv.2017.11.044.

[11] S. Gupta, H.W. Kua, C.Y. Low, Use of biochar as carbon sequestering additive in cement mortar, Cem. Concr. Compos. 87 (2018) 110–129. doi:10.1016/j.cemconcomp.2017.12.009.

[12] S. Gupta, H.W. Kua, S.D. Pang, Biochar-mortar composite: Manufacturing, evaluation of physical properties and economic viability, Constr. Build. Mater. 167 (2018) 874–889. doi:10.1016/j.conbuildmat.2018.02.104.

[13] S. Gupta, H.W. Kua, Effect of water entrainment by pre-soaked biochar particles on strength and permeability of cement mortar, Constr. Build. Mater. 159 (2018) 107–125. doi:10.1016/j.conbuildmat.2017.10.095.

[14] T. Wang, M. Camps-Arbestain, M. Hedley, B.P. Singh, R. Calvelo-Pereira, C. Wang, Determination of carbonate-C in biochars, Soil Res. 52 (2014) 495–504. doi:10.1071/SR13177.

[15] J.H. Yuan, R.K. Xu, H. Zhang, The forms of alkalis in the biochar produced from crop residues at different temperatures, Bioresour. Technol. 102 (2011) 3488–3497. doi:10.1016/j.biortech.2010.11.018.

[16] B. Singh, B.P. Singh, A.L. Cowie, Characterisation and evaluation of biochars for their application as a soil amendment, Soil Res. 48 (2010) 516–525. doi:10.1071/SR10058.

[17] C. Wang, Y. Wang, H.M.S.K. Herath, Polycyclic aromatic hydrocarbons (PAHs) in biochar–Their formation, occurrence and analysis: A review, Org. Geochem. 114 (2017) 1–11. doi:10.1016/j.orggeochem.2017.09.001.

[18] A. Freddo, C. Cai, B.J. Reid, Environmental contextualisation of potential toxic elements and

polycyclic aromatic hydrocarbons in biochar, Environ. Pollut. 171 (2012) 18–24. doi:10.1016/j.envpol.2012.07.009.

[19] M. Achternbosch, K.R. Bräutigam, N. Hartlieb, C. Kupsch, P. Richers, U., Stemmermann, M. Gleis, Heavy metals in cement and concrete resulting from the co-incineration of wastes in cement kilns with regard to the legitimacy of waste utilisation, (2003).

[20] EN 196-1:2016. Methods of testing cement - Part 1: Determination of strength, (2016).

[21] A. Schwartzentruber, C. Catherine, La méthode du mortier de béton équivalent (MBE)—Un nouvel outil d'aide à la formulation des bétons adjuvantés, Mater. Struct. 33 (2000) 475–482. doi:10.1007/s11340-015-0009-1.

[22] EN 1015-3:2007. Methods of test for mortar for masonry. Part 3: determination of consistency of fresh mortar (by flow table), (2007).

[23] EN 1015-6:2007. Methods of test for mortar for masonry. Determination of bulk density of fresh mortar, (2007).

[24] EN 1015-10:2007. Methods of test for mortar for masonry. Determination of dry bulk density of hardened mortar, (2007).

[25] JCI-S-001-2003. Method of test for fracture energy of concrete by use of notched beam, (2003).

[26] J. Blaber, B. Adair, A. Antoniou, Ncorr: Open-Source 2D Digital Image Correlation Matlab Software, Exp. Mech. 55 (2015) 1105–1122. doi:10.1007/s11340-015-0009-1.

[27] R.A. Khushnood, S. Ahmad, L. Restuccia, C. Spoto, P. Jagdale, J.M. Tulliani, G.A. Ferro, Carbonized nano/microparticles for enhanced mechanical properties and electromagnetic interference shielding of cementitious materials, Front. Struct. Civ. Eng. 10 (2016) 209–213. doi:10.1007/s11709-016-0330-5.

[28] S. Ahmad, J.M. Tulliani, G.A. Ferro, R.A. Khushnood, L. Restuccia, P. Jagdale, Crack path and fracture surface modifications in cement composites, Frat. Ed Integrita Strutt. 9 (2015)

524–533. doi:10.3221/IGF-ESIS.34.58.

[29] B. Belletti, P. Bernardi, A. Malcevschi, A. Sirico, Experimental research on mechanical properties of biochar-added cementitious mortars, in: Concr. Innov. Mater. Des. Struct. Proc. Fib Symp. 2019, Kraków, Pol. 27-29 May 2019, FIB-Féd. Int. du Béton., 2019.

[30] L. Restuccia, A. Reggio, G.A. Ferro, R. Kamranirad, Fractal analysis of crack paths into innovative carbon-based cementitious composites, Theor. Appl. Fract. Mech. 90 (2017) 133–141. doi:10.1016/j.tafmec.2017.03.016.

## List of Figures

## List of Tables

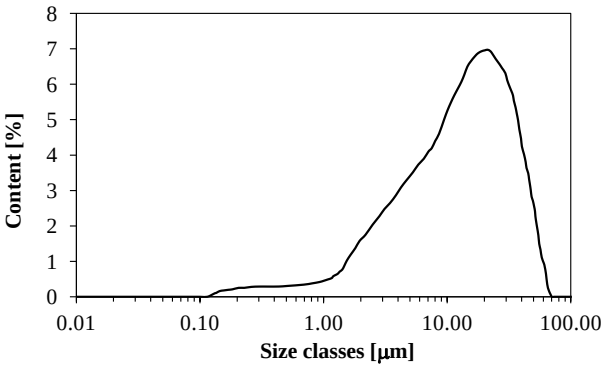


**Figure 1 –** Distribution of biochar particles after sieving through a 63.5 μm mesh.

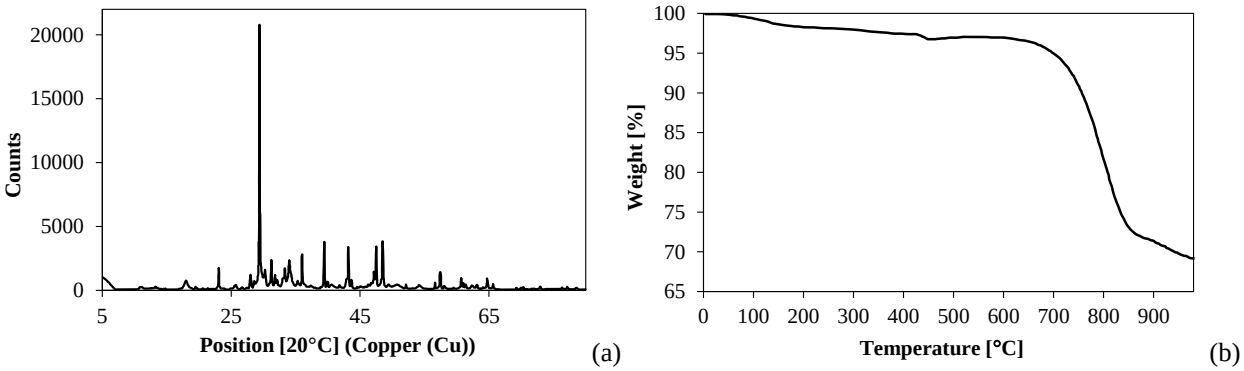


**Figure 2 –** (a) XRD pattern of biochar powder, (b) thermogravimetric analysis (TGA) carried out under nitrogen flow.

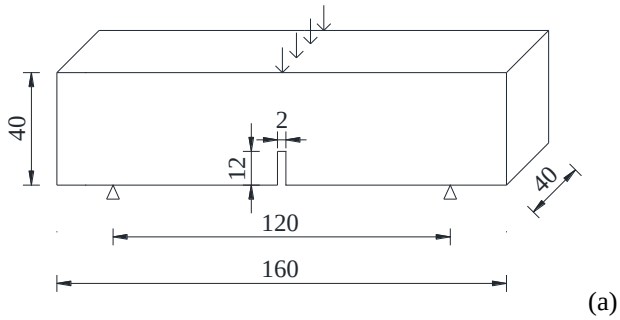


(a)

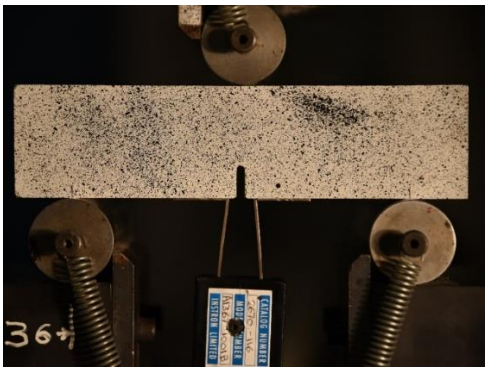

(b)

(c)

(d)

**Figure 3 – (**a) Specimen geometry (in mm), (b) loading configuration of 3PBT, (c) test set up and (d) DIC setup.

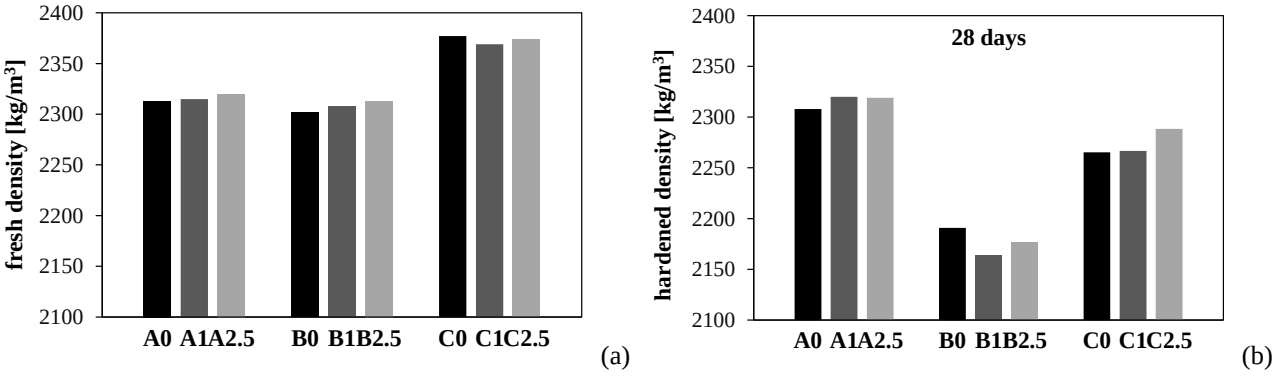


**Figure 4 –** (a) Fresh density and (b) hardened density at 28 days curing of mortar mix A, B and C for the different percentages of biochar investigated.

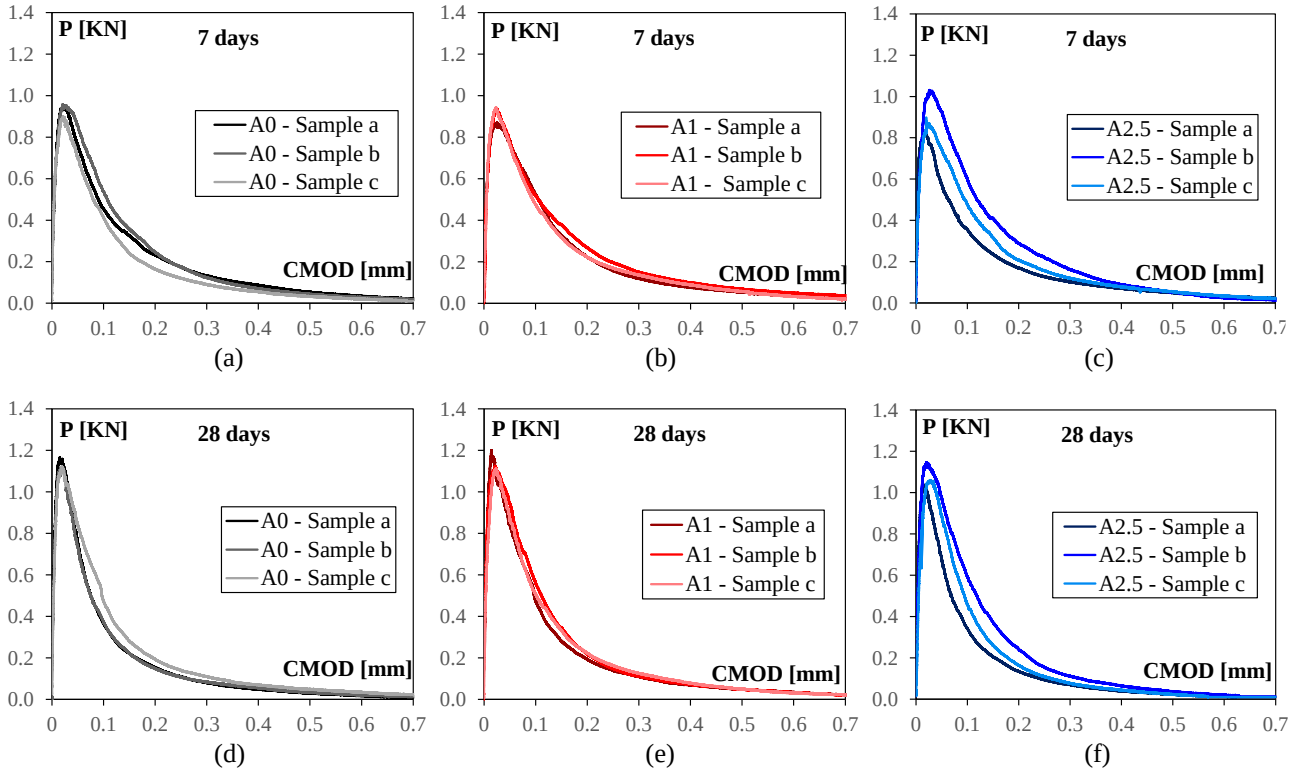


**Figure 5 –** Load - CMOD curves for samples from mix A characterized by different percentages of biochar (a) 0 wt%, (b) 1 wt%, (c) 2.5 wt% at 7 days curing and (d) 0 wt%, (e) 1 wt%, (f) 2.5 wt% at 28 days curing.

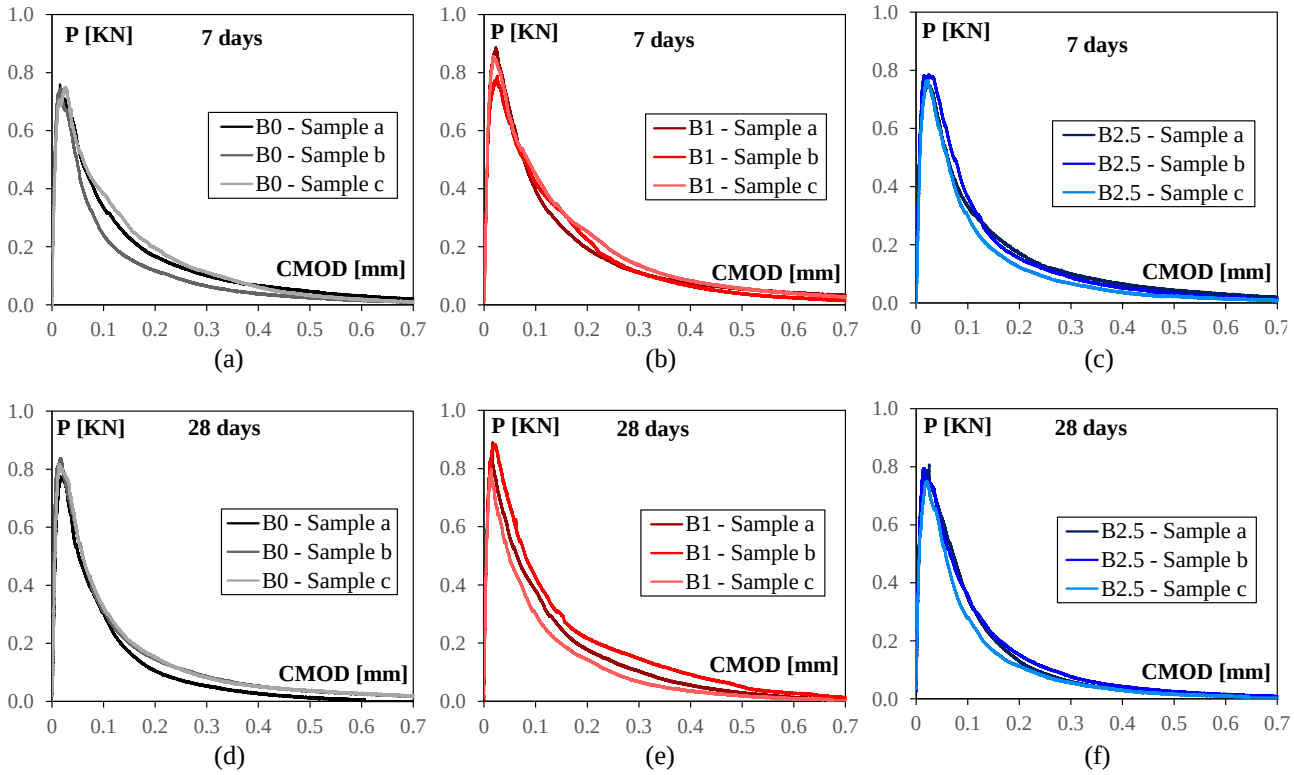


**Figure 6 –** Load - CMOD curves for samples from mix B characterized by different percentages of biochar (a) 0 wt%, (b) 1 wt%, (c) 2.5 wt% at 7 days curing and (d) 0 wt%, (e) 1 wt%, (f) 2.5 wt% at 28 days curing.

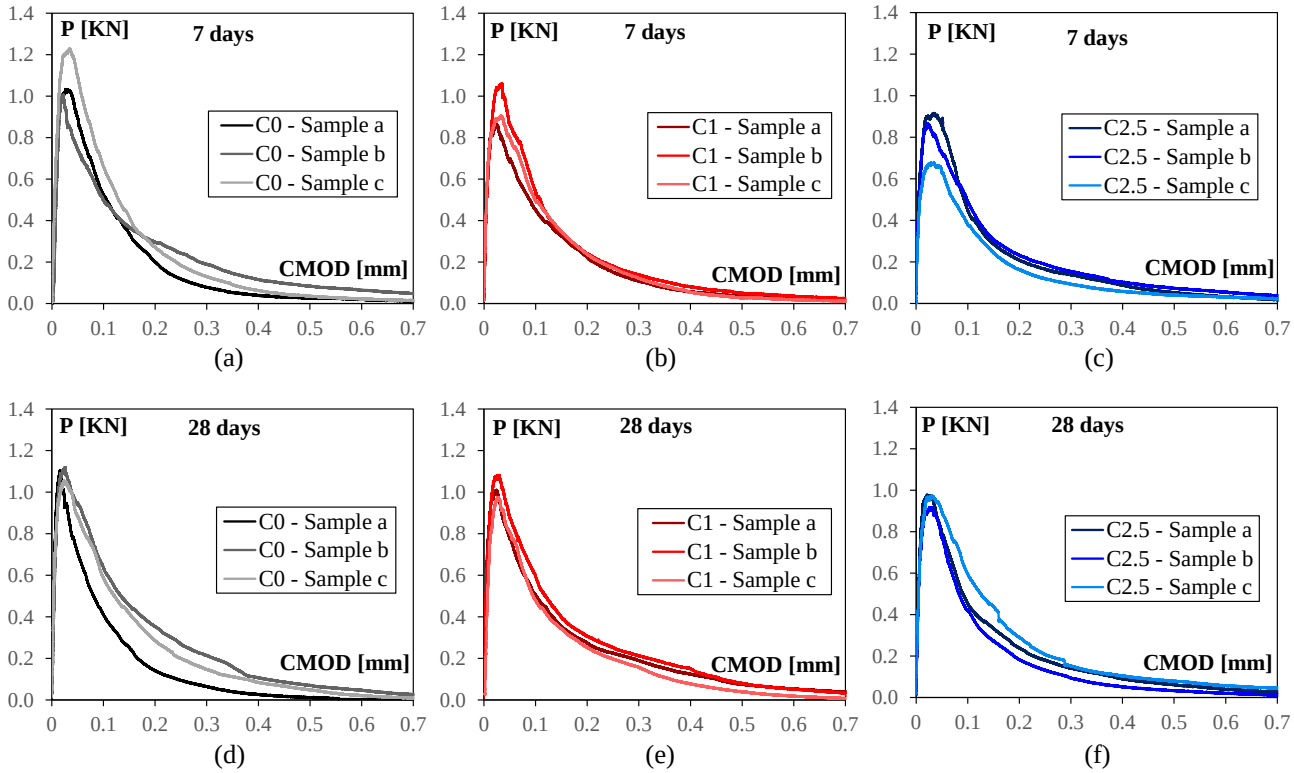


**Figure 7 –** Load - CMOD curves for samples from mix C characterized by different percentages of biochar (a) 0 wt%, (b) 1 wt%, (c) 2.5 wt% at 7 days curing and (d) 0 wt%, (e) 1 wt%, (f) 2.5 wt% at 28 days curing.

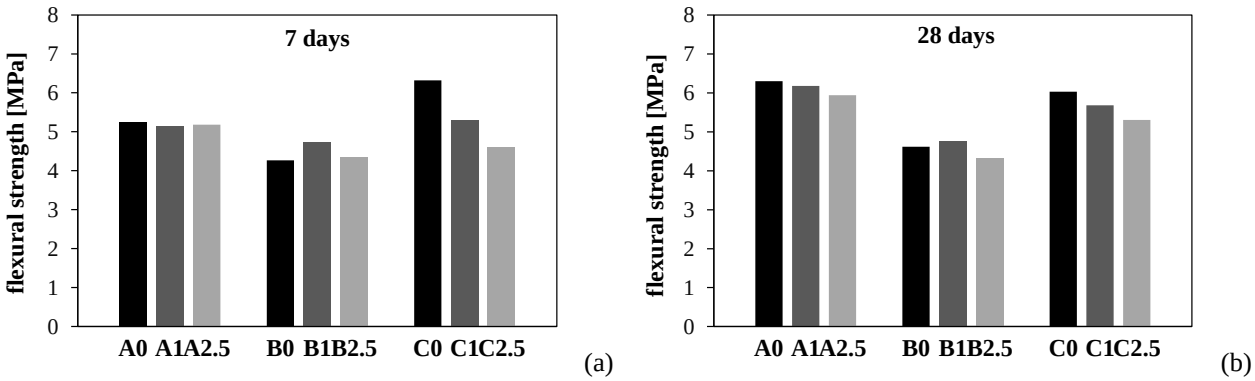


**Figure 8 –** Mean flexural strength of mortar mixes A, B and C, for the different percentages of biochar at (a) 7 and (b) 28 days curing.

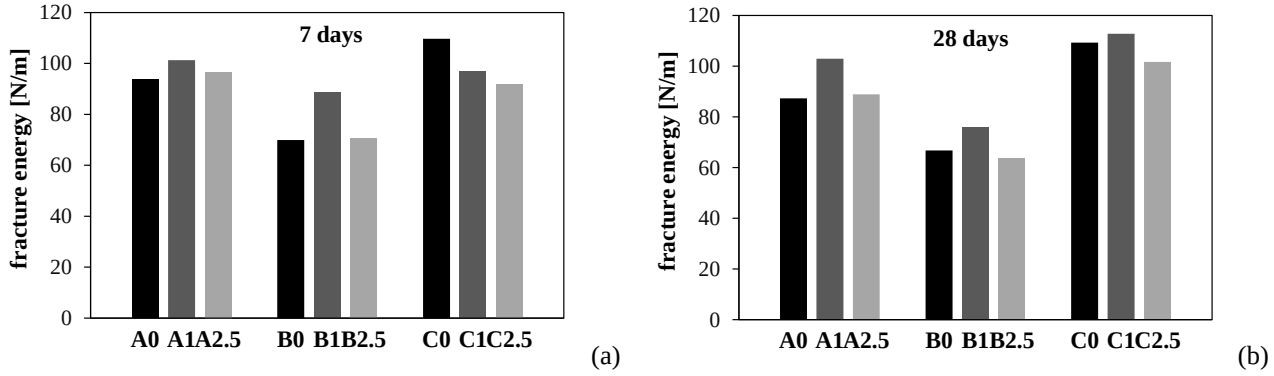


**Figure 9 –** Mean values of fracture energy of mortar mixes A, B and C, for the different percentages of biochar at (a) 7 and (b) 28 days curing.

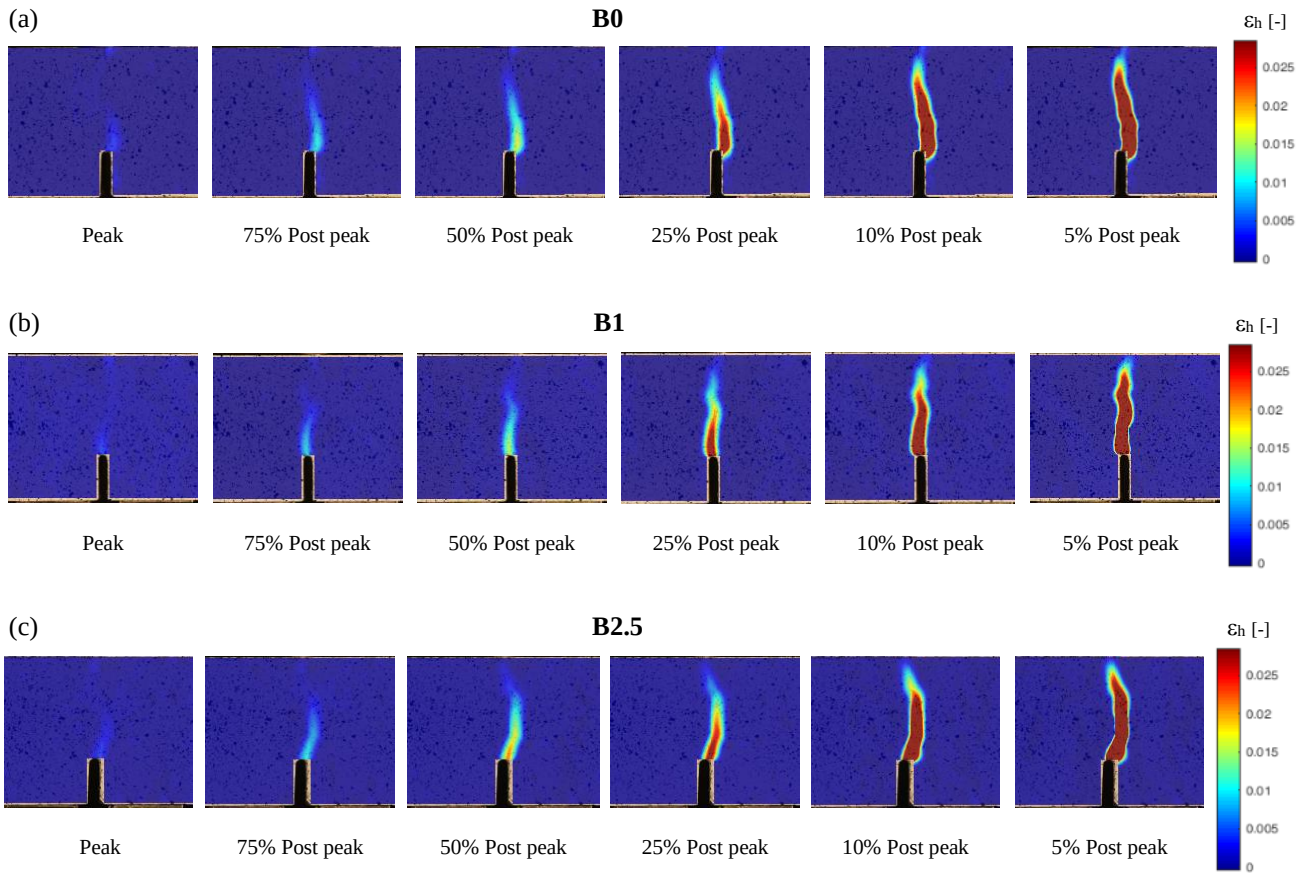


**Figure 10 –** Evolution of cracking in terms of horizontal strain field around the notch from DIC, at different loading stages, for samples of batch B at 28 days curing, for different dosage of biochar: (a) B0 – plain: 0 wt%, (b) B1 – 1 wt%, (c) B2.5 – 2.5 wt%.

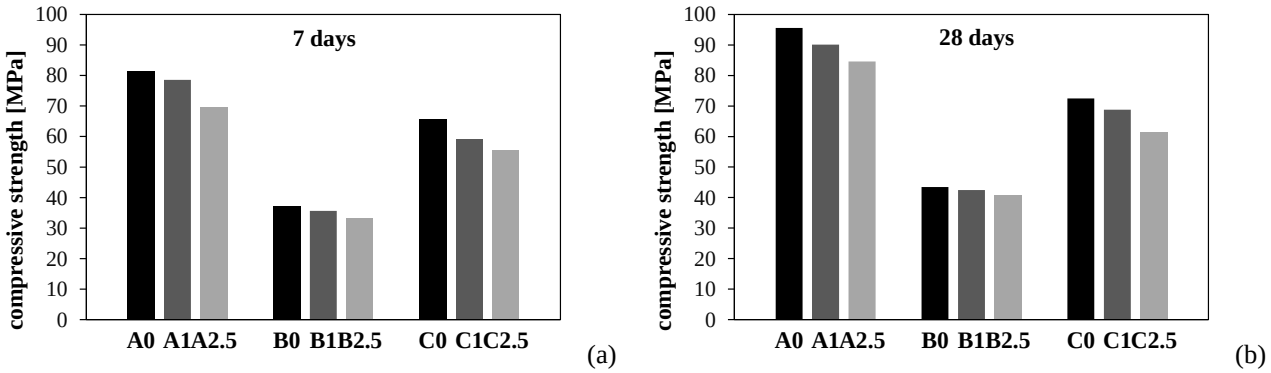


**Figure 11 –** Mean compressive strength of mortar mixes A, B and C, each one characterized by different percentages of biochar (0, 1 and 2.5 wt%) at (a) 7 and (b) 28 days curing.

| **Elemental analysis** | CaO | $K_2O$ | MgO | $P_2O_5$ | $SiO_2$ | MnO | $SO_3$ | $Fe_2O_3$ | $Na_2O$ | BaO | Total |
|---|---|---|---|---|---|---|---|---|---|---|---|
| **XRF %** | 60.49 | 19.25 | 6.16 | 4.17 | 4.15 | 2.38 | 0.98 | 0.55 | 0.42 | 0.2 | 98.75 |

**Table 1** – Biochar chemical composition as obtained from WD-XRF spectrometer.

| **Element** | As | Cd | Cr | Fe | Mg | Hg | Ni | Pb | K | Cu | Na | Zn |
|---|---|---|---|---|---|---|---|---|---|---|---|---|
| **[mg/kg]** | 0.364 | 1.94 | 6.35 | 1310 | 1.52 | <LOD | 59 | 11.3 | 6.07 | 57.2 | 0.115 | 230 |

**Table 2 –** Heavy metal contents (mg/kg) of biochar as obtained from ICP-EOS analysis.

| | Cement | | Aggregates | | Superplasticizer | | Water | Biochar |
|---|---|---|---|---|---|---|---|---|
| | **Type** | **[g]** | **CEN sand** | **0-8 mm** | **Type** | **[g]*** | **W/C ratio** | **%wt of cement** |
| **A0** | I 52.5R | 450 | 1350 | - | Dynamon SP1 | 3.08 | 0.42 | - |
| **A1** | I 52.5R | 450 | 1350 | - | Dynamon SP1 | 3.24 | 0.42 | 1.0 |
| **A2.5** | I 52.5R | 450 | 1350 | - | Dynamon SP1 | 3.85 | 0.42 | 2.5 |
| **B0** | II A-LL 32.5R | 330 | - | 1116 | Dynamon SX42 | 2.64 | 0.55 | - |
| **B1** | II A-LL 32.5R | 330 | - | 1116 | Dynamon SX42 | 2.97 | 0.55 | 1.0 |
| **B2.5** | II A-LL 32.5R | 330 | - | 1116 | Dynamon SX42 | 3.30 | 0.55 | 2.5 |
| **C0** | I 42.5R | 400 | - | 1170 | Dynamon SP1 | 3.00 | 0.40 | - |
| **C1** | I 42.5R | 400 | - | 1170 | Dynamon SP1 | 3.40 | 0.40 | 1.0 |
| **C2.5** | I 42.5R | 400 | - | 1170 | Dynamon SP1 | 3.80 | 0.40 | 2.5 |

***dry content

**Table 3 –** Mix design of the investigated mortars.

| Squared mesh size<br>mm | Cumulated sieve residue<br>% |
|---|---|
| 8.000 | 0.00 |
| 6.300 | 3.01 |
| 4.000 | 28.34 |
| 2.000 | 56.70 |
| 1.000 | 68.90 |
| 0.500 | 75.84 |
| 0.250 | 92.40 |
| 0.125 | 98.40 |
| 0.063 | 99.37 |
| 0.000 | 100.00 |

**Table 4 –** Aggregate size distribution in terms of cumulated sieve residue (%) vs. squared mesh size (mm).

| | Biochar | Water | Superplasticizer* | Flow diameter (mm) - EN 1015-3 | |
|---|---|---|---|---|---|
| | %wt of cement | W/C ratio | %wt of cement | after 0 min | after 25 min |
| **A0** | - | 0.420 | 0.68 | 244 | 176 |
| **A1** | 1.0 | 0.420 | 0.72 | 238 | 173 |
| **A2.5** | 2.5 | 0.420 | 0.86 | 243 | 175 |
| **A1_W** | 1.0 | 0.440 | 0.68 | 246 | 181 |
| **A2.5_W** | 2.5 | 0.455 | 0.68 | 241 | 174 |

***dry content

**Table 5 – S**uperplasticizer and water dosage required for biochar-added mortars type A to maintain the same flowability of the control plain admixture (A0).

| | Biochar | Water | Superplasticizer* | Flow diameter (mm) | | |
|---|---|---|---|---|---|---|
| | %wt of cement | W/C ratio | %wt of cement | after 0 min | after 20 min | after 50 min |
| **B0** | - | 0.55 | 0.80 | 287 | 244 | 219 |
| **B1** | 1.0 | 0.55 | 0.90 | 285 | 233 | 197 |
| **B2.5** | 2.5 | 0.55 | 1.00 | 279 | 195 | 174 |
| **C0** | - | 0.40 | 0.75 | 314 | 250 | 211 |
| **C1** | 1.0 | 0.40 | 0.85 | 308 | 258 | 209 |
| **C2.5** | 2.5 | 0.40 | 0.95 | 286 | 210 | 181 |

***dry content

**Table 6 –** Measure of fresh flowability and corresponding superplasticizer and water dosage adopted for mortars type B and C.